

Spatially Controlled DNA Nanopatterns by “Click” Chemistry Using Oligonucleotides with Different Anchoring Sites

Guangyan Qing,^{†,§,¶} Hai Xiong,^{†,+,¶} Frank Seela,^{*,‡,+} and Taolei Sun^{*,†,§}

State Key Laboratory of Advanced Technology for Materials Synthesis and Composite, Wuhan University of Technology, Wuhan 430070, China, Laboratory of Bioorganic Chemistry and Chemical Biology, Center for Nanotechnology, D-48149 Münster, Germany, Physikalisches Institut, WWU Münster, D-48149 Münster, Germany, and Laboratorium für Organische und Biorganische Chemie, Institut für Chemie, Universität Osnabrück, D-49069 Osnabrück, Germany

Received June 15, 2010; E-mail: sunt@uni-muenster.de; seela@uni-osnabrueck.de

Abstract: DNA patterning on surfaces has broad applications in biotechnology, nanotechnology, and other fields of life science. The common patterns make use of the highly selective base pairing which might not be stable enough for further manipulations. Furthermore, the fabrication of well-defined DNA nanostructures on solid surfaces usually lacks chemical linkages to the surface. Here we report a template-free strategy based on “click” chemistry to fabricate spatially controlled DNA nanopatterns immobilized on surfaces. The self-assembly process utilizes DNA with different anchoring sites. The position of anchoring is of crucial importance for the self-assembly process of DNA and greatly influences the assembly of particular DNA nanopatterns. It is shown that the anchoring site in a central position generates tunable nanonetworks with high regularity, compared to DNAs containing anchoring sites at terminal and other positions. The prepared patterns may find applications in DNA capturing and formation of pores and channels and can serve as templates for the patterning using other molecules.

DNA patterning on surface find applications in chemistry, physics, and biology, including biotechnology,¹ nanotechnology,² etc.³ Existing work describing the fabrication of well-defined DNA nanostructures⁴ and patterns on solid surfaces is based on the highly specific Watson–Crick or Hoogsteen base pairing between two or more DNA strands.⁵ However, the obtained patterns usually lack chemical bonds with the substrate, which may not be stable enough for further manipulations. The Huisgen–Meldal–Sharpless “click” reaction⁶ has emerged as a convenient and effective protocol to immobilize DNA and other biomolecules onto surfaces.^{7,8} Here we report a template-free strategy based on “click” chemistry to fabricate spatially

controlled DNA nanopatterns immobilized on surfaces utilizing the self-assembly process of DNA with different anchoring sites.

The introduction of terminal triple bonds into the side chains of all four DNA constituents has been reported.⁹ Recently, we¹⁰ developed a novel 2'-deoxyribonucleoside building block of 8-aza-7-deaza-7-(octa-1,7-diynyl)-2'-deoxyguanosine (dG*). This dG-analogue contains a pyrazolo[3,4-d]pyrimidine instead of a purine and a hydrophobic side chain acting as spacer and a terminal triple bond as a clickable unit. Oligonucleotides used in this study contain the modified 2'-deoxyguanosine dG* unit to anchor DNA onto a solid surface. Different from conventional methods, which make use of triple bonds that are present in

[†] Wuhan University of Technology.

[‡] Center for Nanotechnology.

[§] Physikalisches Institut.

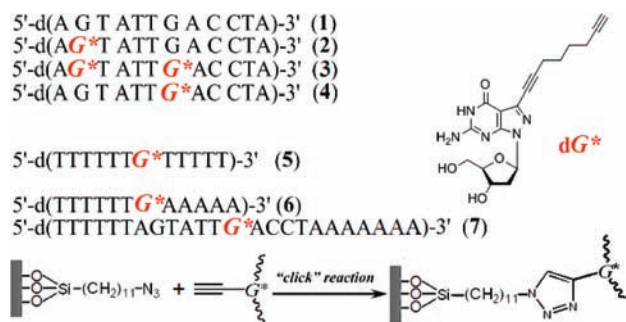
[¶] Universität Osnabrück.

^{*} These authors contributed equally to this work.

- (1) Wiradharma, N.; Tong, Y. W.; Yang, Y. Y. *Biomaterials* **2009**, *30*, 3100.
- (2) For example:(a) Yan, H.; Park, S. H.; Finkelstein, G.; Reif, J. H.; LaBean, T. H. *Science* **2003**, *301*, 1882. (b) He, Y.; Ye, T.; Su, M.; Zhang, C.; Ribbe, A. E.; Jiang, W.; Mao, C. *Nature* **2008**, *452*, 198. (c) Endo, M.; Sugiyama, H. *ChemBioChem* **2009**, *10*, 2420.
- (3) (a) Liu, Y.; Lin, C.; Li, H.; Yan, H. *Angew. Chem., Int. Ed.* **2005**, *44*, 4333. (b) Zhang, J.; Narayan, R. J. *NanoScience in Biomedicine*; Shi, D., Ed.; Springer: New York, 2009; pp 405427.
- (4) For example:(a) Seeman, N. C. *Nature* **2003**, *421*, 427. (b) Aldaye, F. A.; Palmer, A. L.; Sleiman, H. F. *Science* **2008**, *321*, 1795.
- (5) (a) Sun, X.; Hyeon Ko, S.; Zhang, C.; Ribbe, A. E.; Mao, C. *J. Am. Chem. Soc.* **2009**, *131*, 13248. (b) Lin, C.; Liu, Y.; Yan, H. *Biochemistry* **2009**, *48*, 1663. (c) Costa, L. T.; Kerkmann, M.; Hartmann, G.; Endres, S.; Bisch, P. M.; Heckl, W. M.; Thalhammer, S. *Biochem. Biophys. Res. Commun.* **2004**, *313*, 1065.

- (6) (a) Kolb, H. C.; Finn, M. G.; Sharpless, K. B. *Angew. Chem., Int. Ed.* **2001**, *40*, 2004. (b) Iha, R. K.; Wooley, K. L.; Nyström, A. M.; Burke, D. J.; Kade, M. J.; Hawker, C. J. *Chem. Rev.* **2009**, *109*, 5620. (c) El-Sagheer, A. H.; Brown, T. *Chem. Soc. Rev.* **2010**, *39*, 1388. (d) Seo, T. S.; Bai, X.; Ruparel, H.; Li, Z.; Turro, N. J.; Ju, J. *Proc. Natl. Acad. Sci. U.S.A.* **2004**, *101*, 5488. (e) Hawker, C. J.; Wooley, K. L. *Science* **2005**, *309*, 1200.
- (7) (a) Jonkheijm, P.; Weinrich, D.; Schröder, H.; Niemeyer, C. M.; Waldmann, H. *Angew. Chem., Int. Ed.* **2008**, *47*, 9618. (b) Rozkiewicz, D. I.; Gierlich, J.; Burley, G. A.; Gutmiedl, K.; Carell, T.; Ravoo, B. J.; Reinhoudt, D. N. *ChemBioChem* **2007**, *8*, 1997. (c) Rozkiewicz, D. I.; Brugman, W.; Kerkhoven, R. M.; Ravoo, B. J.; Reinhoudt, D. N. *J. Am. Chem. Soc.* **2007**, *129*, 11593.
- (8) (a) Schlossbauer, A.; Schaffert, D.; Kecht, J.; Wagner, E.; Bein, T. *J. Am. Chem. Soc.* **2008**, *130*, 12558. (b) Sumerlin, B. S.; Vogt, A. P. *Macromolecules* **2010**, *43*, 1. (c) Amblard, F.; Cho, J.-H.; Schinazi, R. F. *Chem. Rev.* **2009**, *109*, 4207.
- (9) (a) Seela, F.; Sirivolu, V. R.; Chittepu, P. *Bioconjugate Chem.* **2008**, *19*, 211. (b) Seela, F.; Sirivolu, V. R. *Chem. Biodiversity* **2006**, *3*, 509.
- (10) Seela, F.; Xiong, H.; Leonard, P.; Budow, S. *Org. Biomol. Chem.* **2009**, *7*, 1374.

Scheme 1. Oligonucleotide Sequences Used in This Study and the Click Reaction to Anchor DNA onto the Solid Surface^a



^a dG* refers to the modified dG with a terminal triple bond.

terminal linkers, the triple bond anchoring site of dG* can be introduced at any position of an oligonucleotide chain. Here we show that the position of such a dG* anchor containing a lipophilic side chain greatly influences the self-assembly process of DNA, and thus is of crucial importance for the generation of the particular DNA nanopatterns. It is further shown that the dG* in a central position generates tunable nanonetworks with high regularity, compared to DNAs containing dG* in terminal and other positions.

For this study, we selected different oligonucleotides (ODNs), shown in Scheme 1. The 12-mer oligonucleotide 5'-d(AGTATTGACCTA) (1) was used as a reference compound.¹¹ Through substituting one or two dG bases by dG* units, we introduced different anchoring sites in the DNA strand (Scheme 1, ODNs 2–4). ODN-5 represents a homomeric dT with a central dG* unit, whereas ODN-6 is related to this structure but composed of blocks of dT and dA elements being self-complementary with a central anchor of dG*. While ODN-4 exists as single strand, ODN-7 contains self-complementary elements at both sides of it, which can form Watson–Crick base pairs resulting in double-stranded dA–dT regions (duplexes or hairpins).

The silicon wafer was premodified with a mixture of 11-bromo-undecyltrimethoxysilane (BUTS) and triethoxyoctylsilane (TEOS) (molar ratio is 3:7) followed by nucleophilic displacement of the bromo substituent with azide (NaN₃) to yield the reactive self-assembled monolayer (SAM) with terminal azido groups.¹² Then, the silicon wafer was immersed in oligonucleotide solutions containing all the necessary components to perform the copper(I)-catalyzed azide–alkyne cycloaddition reaction (click reaction, see Scheme 1).¹³ After gentle shaking at room temperature for several hours, the substrate was washed with ethanol, hexane, and water successively and repeatedly to remove unbound DNA and the catalyst. Thereafter, it was dried by a flow of nitrogen and then analyzed by atomic force microscopy (AFM).

Figure 1a shows the AFM image for the premodified silicon wafer surface containing only the azide functionalities. The

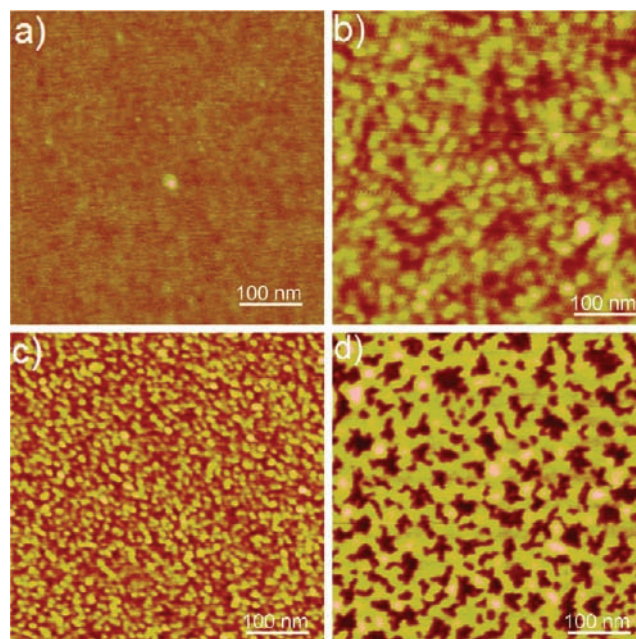


Figure 1. AFM images of the DNA-coated silicon wafer by click chemistry. (a) Undecylazide/octyl premodified silicon wafer. (b) ODN-2 (5'-d(AG*TATTGACCTA)-3'). (c) ODN-3 (5'-d(AG*TATTG*ACCTA)-3'). (d) ODN-4 (5'-d(AGTATTG*ACCTA)-3').

surface appears quite smooth. Two control experiments (one is the premodified surface with ODN-1 without dG* unit, the other is the unmodified surface with ODN-4 having the dG* unit) gave similar pictures (see Supporting Information (SI)). This indicates that the DNA molecules were not immobilized onto the surface in the absence of the click reaction and were removed easily during the washing process. Figure 1b is a typical AFM image of the DNA SAM film obtained from the click reaction with ODN-2 incorporating the dG* modification at a terminal position. It shows a densely packed particle morphology (Figure 1b) with narrowly distributed diameters of 20–30 nm. A similar particle morphology was observed for ODN-3 with terminal and an additional central dG* modification sites. However, in this case, a more densely packed morphology is observed and the particle size is much smaller, ranging between 10–15 nm (Figure 1c). Interestingly, for ODN-4 with the central modified dG* residue, we got a totally different pattern composed of nanonetwork structures with sizes of 30–50 nm and depth of 1.5–2.6 nm (Figure 1d). Such a pattern is not an occasional phenomenon. It is found on the whole surface uniformly (see Figure 2a for the large-scale AFM image). Considering that the drying process may have influence on the nanostructure formation, we also used ethanol and hexane, respectively, as the last solvent before the drying process and the subsequent AFM imaging. The obtained patterns (for hexane treatment, see Figure 2b; for ethanol treatment, see SI) are identical to each other. It shows that the pattern is quite stable and the pattern formation is not related to the washing process.

The above results indicate that the dG* anchoring sites are of crucial importance for the DNA self-assembly on surfaces. Since the feature sizes of patterns in Figure 1d are much larger than the molecular dimensions of DNA, these patterns must represent complexes of multiple (tens of) DNA strands. Normally, the DNA self-assembly process is primarily driven by hydrogen bonding (base pairing) controlled by the se-

- (11) (a) He, J.; Seela, F. *Nucleic Acids Res.* **2002**, *30*, 5485. (b) Seela, F.; Peng, X.; Li, H. *J. Am. Chem. Soc.* **2005**, *127*, 7739.
 (12) (a) Lummerstorfer, T.; Hoffmann, H. *J. Phys. Chem. B* **2004**, *108*, 3963. (b) Fryxell, G. E.; Rieke, P. C.; Wood, L. L.; Engelhard, M. H.; Williford, R. E.; Graff, G. L.; Campbell, A. A.; Wiacek, R. J.; Lee, L.; Halverson, A. *Langmuir* **1996**, *12*, 5064. (c) Heise, A.; Menzel, H.; Yim, H.; Foster, M. D.; Wieringa, R. H.; Schouten, A. J.; Erb, V.; Stamm, M. *Langmuir* **1997**, *13*, 723.
 (13) (a) Devaraj, N. K.; Miller, G. P.; Ebina, W.; Kakaradov, B.; Collman, J. P.; Kool, E. T.; Chidsey, C. E. D. *J. Am. Chem. Soc.* **2005**, *127*, 8600. (b) Rostovtsev, V. V.; Green, L. G.; Fokin, V. V.; Sharpless, K. B. *Angew. Chem., Int. Ed.* **2002**, *41*, 2596. (c) Lee, J. K.; Chi, Y. S.; Choi, I. S. *Langmuir* **2004**, *20*, 3844.

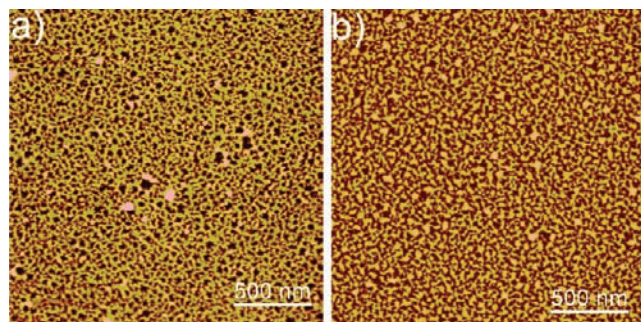
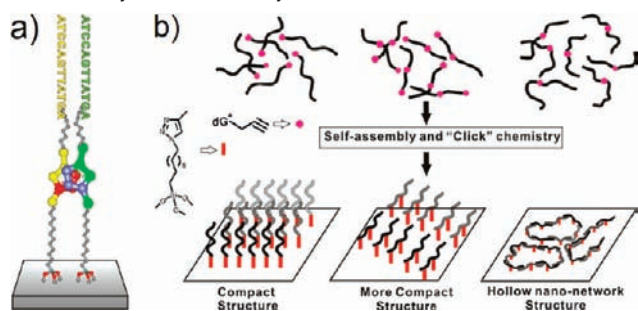


Figure 2. Large-scale AFM image obtained from ODN-4 (5'-d-(AGTATTG*ACCTA)-3') using water (a) or hexane (b) as the last solvent before the drying process and AFM imaging. They are almost identical to each other. Considering the same result for ethanol treatment (see SI), it indicates that the pattern formation is not related to the washing procedure.

Scheme 2. Potential Mechanism for the DNA Nanostructure Formation by Click Chemistry^a



^a (a) Aromatic stacking between the 1,2,3-s-triazole moieties of two neighbouring oligonucleotides. (b) Schematic diagram of the self-assembly fashions for oligonucleotides with terminal (ODN-2: 5'-d(AG*TATTGACCTA)-3'), middle (ODN-4: 5'-d(A GTATTG*ACCTA)-3') and both (ODN-3: 5'-d(AG*TATTG*ACCTA)-3') dG* modifications, respectively, in which the black wave lines represent the DNA strands.

quence,¹⁴ and stacking interaction between nucleobases,¹⁵ as well as the interplay of hydrophilic character of the backbone and the hydrophobic properties of the nucleobases.¹⁶ Since Watson–Crick base pairs are not formed between noncomplementary strands, such as ODN-2, ODN-3, and ODN-4, other factors have to be responsible for the various assemblies formed by single-stranded DNAs. The principle differences between the various immobilization processes and the morphological consequences are outlined in Scheme 2b. Stacking interactions of the 1,2,3-s-triazole moieties formed during the click immobilization as well as hydrophobic interaction of the side chains used as linker have to be taken into account (Scheme

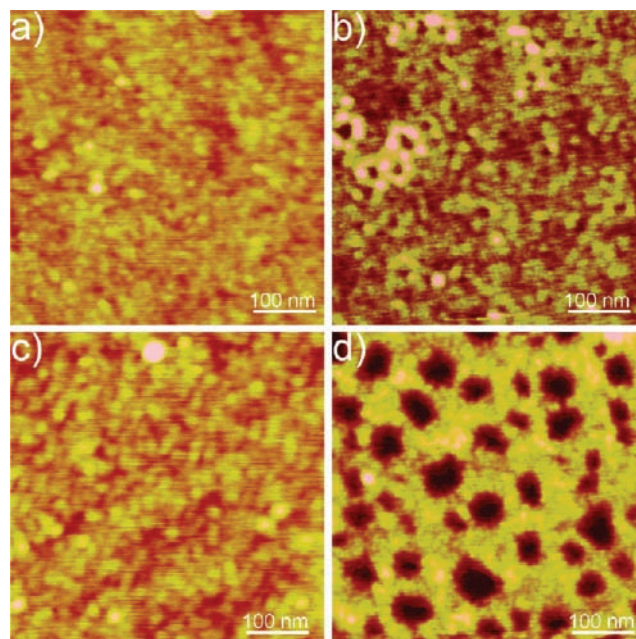


Figure 3. Influence of the surface density for azide moieties on the DNA self-assembly nanostructures. (a)–(c) show the typical AFM images for self-assembly DNA nanostructures of ODN-4 (5'-d(AGTATTG*ACCTA)-3') obtained from the premodified silicon substrates with BUTS:TEOS ratios of 1:9, 6:4, and 10:0, respectively. (d) is the AFM image obtained from ODN-5 sequence (5'-d(TTTTGG*TTTT)-3') on silicon substrate with medium BUTS:TEOS ratio of 3:7. For corresponding large-scale images, see SI.

2a). Both can hold oligonucleotide strands together.¹⁷ As repulsive forces of the negatively charged backbone (phosphodiester residues) which may hinder aggregation are neutralized by counterions, multistranded assemblies can be formed.^{14b,18} Moreover, single strands of ODN-2 and ODN-3 are flexible and can form compact self-assembled structures more easily than stiff oligonucleotide duplexes. More compact packing of ODN-3 is caused by the two anchoring sites within one molecule. However, for ODN-4, the situation is rather different. The central dG* modification causes a branched structure with regard to the immobilization site with two flexible oligonucleotide arms and hydrophobic side chains linked to the modified surface. From the structural point of view—steric demand and repulsive forces of residues—the formation of a compact structure is unlikely, compared to that of the linear oligonucleotides with terminal dG* residue. The porous nanonetwork structure shown in Figure 1d is formed, which is a result of the minimum energy distribution.

As all these interactions are controlled by the distance of oligonucleotides, the surface density of azido groups on the silicon wafer may affect the patterning. In order to address this point, we changed the ratio of BUTS:TEOS during the pre-modification process of silicon wafer and imaged the resulting patterns after click reaction with ODN-4. Figure 3a–c show the AFM images obtained from BUTS:TEOS ratios of 1:9, 6:4, and 10:0, respectively. Considering the results reported above (BUTS:TEOS, 3:7), we observed an interesting transition

- (14) (a) Moody, E. M.; Bevilacqua, P. C. *J. Am. Chem. Soc.* **2003**, *125*, 16285. (b) Sinden, R. R. *DNA Structure and Function*; Academic Press: San Diego, CA, 1994. (c) Manalo, M. N.; Pérez, L. M.; LiWang, A. *J. Am. Chem. Soc.* **2007**, *129*, 11298.
- (15) (a) Holmlin, R. E.; Dandliker, P. J.; Barton, J. K. *Angew. Chem., Int. Ed.* **1997**, *36*, 2714. (b) Kelley, S. O.; Barton, J. K. *Science* **1999**, *283*, 375. (c) Tashiro, R.; Sugiyama, H. *Angew. Chem., Int. Ed.* **2003**, *42*, 6018. (d) Matta, C. F.; Castillo, N.; Boyd, R. J. *J. Phys. Chem. B* **2006**, *110*, 563. (e) Rebek, J., Jr.; Williams, K.; Parris, K.; Ballester, P.; Jeong, K.-S. *Angew. Chem., Int. Ed.* **1987**, *26*, 1244.
- (16) (a) Tanford, C. *The Hydrophobic Effect*, 2nd ed.; John Wiley: New York, 1980. (b) Tang, K.; Gan, H.; Li, Y.; Chi, L.; Sun, T.; Fuchs, H. *J. Am. Chem. Soc.* **2008**, *130*, 11284. (c) Gan, H.; Tang, K.; Sun, T.; Hirtz, M.; Li, Y.; Chi, L.; Butz, S.; Fuchs, H. *Angew. Chem., Int. Ed.* **2009**, *48*, 5282.

- (17) (a) Dupouy, G.; Marchivie, M.; Triki, S.; Sala-Pala, J.; Salaün, J.-Y.; Gómez-García, C. J.; Guionneau, P. *Inorg. Chem.* **2008**, *47*, 8921. (b) Zhang, K. L.; Qiao, N.; Gao, H. Y.; Zhou, F.; Zhang, M. *Polyhedron* **2007**, *26*, 2461.
- (18) Berg, J. M.; Tymoczko, J. L.; Stryer, L. *Biochemistry*, 6th ed.; W.H. Freeman: New York, 2006.

process of the DNA nanostructure for the central dG^* modified ODN-4 while increasing the BUTS amount, i.e. the surface proportion of the azido groups. For a low ratio (1:9), the AFM image exhibits a loosely packed particle morphology (Figure 3a). When the ratio increases to 3:7, a nanonetwork pattern appears (Figure 1d). However, for the higher ratio of 6:4, this structure shrinks significantly to small nanocircles (Figure 3b) with sizes of 20–30 nm. It indicates that the higher surface density of azido groups reduces the distance between DNA chains, which improves dipole–dipole and π – π stacking interactions between the 1,2,3-s-triazole moieties, as well as hydrophobic interaction among the linkers which compresses the self-assembled nanonetwork. When the BUTS proportion further increases to 100%, the structure changes completely to a closely packed particle-like morphology (Figure 3c) that is very similar to that formed by the terminal functionalized ODN-2 (BUTS: TEOS, 3: 7) shown in Figure 1b. On the other hand, we did not observe such phenomenon when using ODN-2 and ODN-3. This indicates that the central dG^* substitution and the appropriate graft density are crucial to generate well-defined DNA nanonetwork structures on a surface. This point was further proved by experiments using oligonucleotide ODN-5 containing dT blocks at both sides of dG^* residue (Scheme 1). At medium BUTS ratio (30%), a marked nanohole network structure is observed (Figure 3d).

It has been found that base pairing is an important feature to fabricate precisely controlled DNA self-assembled nanostructures.^{4,19} Therefore, we designed another set of oligonucleotides (ODN-6 and ODN-7, see Scheme 1) with complementary dA and dT elements flanking the dG^* residue (ODN-6) or flanking the terminals of ODN-4. In contrast to ODN-1–5, ODN-6 and 7 can form base pairs by hydrogen bonding and base stacking within double-stranded region. Then the same click experiments were performed using a medium 3:7 ratio for silicon wafer immobilization. As shown in Figure 4a, ODN-6 gives a much more regular porous nanonetwork than ODN-4. The pores exhibit a roughly circular morphology with uniform diameters around 20 nm and depth around 1.5 nm with a thin wall of about 10 – 15 nm in thickness. The actual thickness may be much smaller due to the lateral magnification effect of the AFM tip, which may represent one or two parallel duplex structures according to our experience. In this case, each circular structure may involve 20–30 ODN-6 strands (it is roughly determined according to the perimeter of the nanopores, and the length contribution of about 2–3 nm for each strand to form duplex structure due to the base-pairing). ODN-7 (Figure 4b) also gives a similar porous nanonetwork structure; however, the pore sizes are approximately twice (~ 40 nm) as those for ODN-6. Their depth is also a little higher, which is around 2.4 nm, while the thickness of the walls between them remains the same as that of ODN-6. Each nanopore may also involve similar numbers of ODN-7 strands, since the base number of ODN-7 is twice as that of ODN-6. Considering that ODN-6 and ODN-7 have the same complementary tails but a different number of nucleoside residues in the single-stranded connector region, it results in an interplay of base paired elements with nonbase pairing regions which can lead to larger pattern (Figure 4d left). Apparently, a combination of a flexible region (single strand) containing the anchoring site with stiff base paired elements can lead to a novel nanopattern not accessible by pure single-stranded or duplex DNA. We anticipate that larger or other

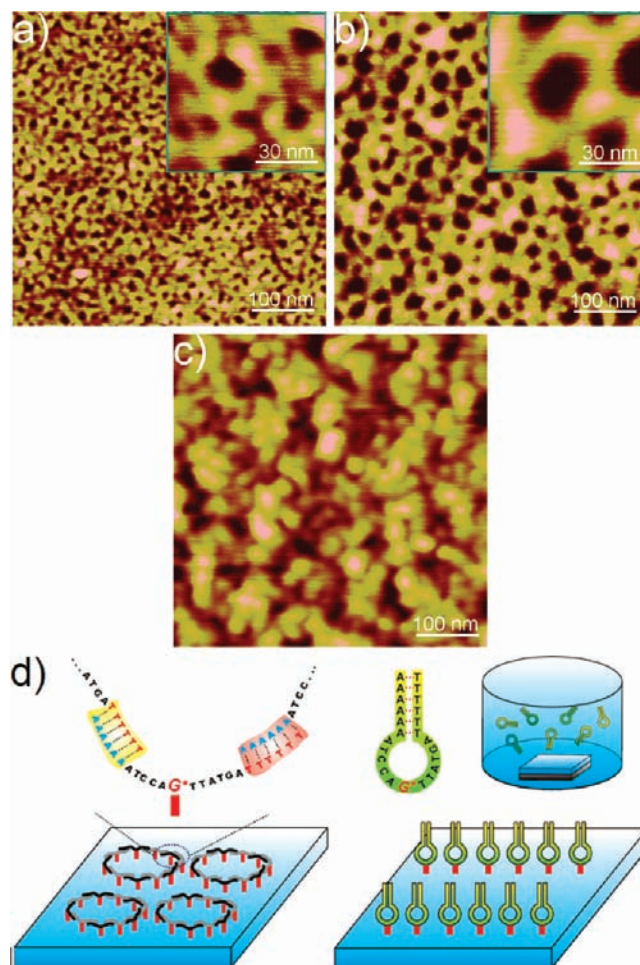


Figure 4. AFM images of (a) oligonucleotides ODN-6 (5'-d(TTTTTT G^* AAAA)-3') and (b) ODN-7 (5'-d(TTTTTTAGTATT G^* ACCTAAAAAAA)-3'), at a surface undecylazide content of 30%. Insets are magnified AFM images of the pores. (c) AFM image for the control experiment using ODN-7 with the addition of 1 M NaCl. (d) Schematic diagram for the different surface self-assembly processes of ODN-7 without (left) or with (right) the presence of NaCl in DNA solution, which give rise to the formation of the duplex or nanohairpin structure between neighboring DNA molecules on surface, respectively.

shapes of regular network structures can be formed through designing the exact sequence of nucleotides containing the dG^* unit and the complementary elements.

Another experiment was performed, in which NaCl was added into the ODN-7 solution before the grafting process to give a final salt concentration of 1 M. Under these conditions, ODN-7 forms a hairpin in solution with a dA = dT stem, a noncomplementary loop, and a central dG^* residue, as verified by concentration-independent melting T_m values (for details, see SI).²⁰ We anticipated that a porous nanostructure would not be formed in the case of hairpin formation because intermolecular hybridization will be prohibited and the DNA nanohairpin might behave as the terminal dG^* -modified nucleotide (like ODN-2) (Figure 4d, right). As shown in Figure 4c, only large particle-like morphology with feature size of 30–50 nm was obtained for the self-assembled film. However, at low salt concentration, duplex or hairpin are destabilized in solution. In contrary,

(19) Mitchell, J. C.; Harris, J. R.; Malo, J.; Bath, J.; Turberfield, A. J. *J. Am. Chem. Soc.* **2004**, *126*, 16342.

(20) (a) Chou, S.-H.; Chin, K.-H.; Wang, A. H.-J. *Nucleic Acids Res.* **2003**, *31*, 2461. (b) Leunissen, M. E.; Dreyfus, R.; Cheong, F. C.; Grier, D. G.; Sha, R.; Seeman, N. C.; Chaikin, P. M. *Nat. Mater.* **2009**, *8*, 590.

hybridization can occur at the surface as the oligonucleotide concentration is increased compared to that of the solution. In that case, duplex formation (Figure 4d left) is favored over hairpin structures. It provides another evidence verifying the self-assembly mechanism proposed in Scheme 2.

One might ask how an oligonucleotide which is fixed covalently to the surface can form nanopatterns, and is the DNA nanoassembly already formed in solution²¹ or only on the surface. In order to clarify this point we used dynamic light scattering (DLS) to detect the self-assembled DNA already in aqueous solution. However, in this experiment, there is not any indication for the formation of assembled DNA in a range of 10–100 nm for ODN-1 to ODN-7. Therefore, it can be inferred that the self-assembly and immobilization processes occur simultaneously on the surface and may mutually promote and interact with each other, which finally give rise to different nanostructures and patterns according to the mechanism proposed above.

In conclusion, we report a click chemistry-based strategy to fabricate DNA self-assembly nanostructures and patterns chemically bound onto a solid surface. Utilizing a dG* unit bearing terminal triple bonds, which can be incorporated into the DNA sequences at any position according to the sequence design, the oligonucleotides can be conveniently grafted chemically onto a solid surface functionalized with azido groups via the click reaction. Our study indicates that the dG* positioning greatly influences the self-assembly process of the oligonucleotides and thus results in different DNA surface nanostructures. Especially, the central dG* position can offer two flexible DNA arms that allow the DNA self-assembly by hybridization of the flanking elements, resulting in nanonetwork structures with high regularity, which is tunable according to the exact sequence and the dG* position. Due to the easy tunability and high stability of the DNA nanopatterns on surfaces, our method may help to extend applications of nanoarchitectures and to construct further DNA nanodevices on surfaces. This includes the construction of DNA pores and channels, which have the potential to capture or deliver DNA and for diagnostic purposes, DNA sequencing, or nanomedical applications, etc.

Experimental Section

Synthesis and Purification of the Oligonucleotides 2–7. The syntheses of oligonucleotides were performed on a DNA synthesizer, model 392-08 (Applied Biosystems, Weiterstadt, Germany) at 1 μ mol scale following the synthesis protocol for 3'-O-(2-cyanoethyl)phosphoramidites.¹⁰ After cleavage from the solid support, the oligonucleotides were deprotected in 25% aqueous ammonia solution for 12–16 h at 60 °C. The purification of the 'trityl-on' oligonucleotides was carried out on reversed-phase HPLC (Merck-Hitachi-HPLC; RP-18 column; gradient system (A = MeCN, B = 0.1 M (Et₃NH)OAc (pH 7.0)/MeCN, 95:5); 3 min 15% A in B, 12 min 15–50% A in B, and 5 min 50–10% A in B; flow rate 1.0 cm³/min. The purified 'trityl-on' oligonucleotides were treated with 2.5% CHCl₂COOH/CH₂Cl₂ for 5 min at 0 °C to remove the 4,4'-dimethoxytrityl residues. The deprotected oligomers were purified again by reversed-phase HPLC (gradient: 0–25 min 0–20% A in B; flow rate 1.0 mL/min). The oligomers were desalted on a short column (RP-18) and lyophilized on a Speed-Vac

evaporator to yield colorless solids which were frozen at –24 °C. The molecular masses of the oligonucleotides 2–7 were determined by MALDI-TOF mass spectrometry (see SI) in the linear negative mode.

Preparation of the Azide-Terminated Silicon Substrates. Cleaned silica wafers were immersed in aqueous NaOH (0.1 M) for 5 min and subsequently in HNO₃ (0.1 M) for 10 min to generate surface hydroxyl groups. After being washed with an excess of water and dried by N₂ flow, they were placed in a solution of 1.2 vol% 11-bromo-undecyl-trimethoxysilane (BUTS) and 2.8 vol% triethoxyoctylsilane (TEOS) (the proportion of BUTS/TOS can be adjusted according to different requirements, while their total concentration remains the same) in dry toluene (10 mL) at 20 °C for 24 h. The wafers were then soaked for 5 min and sonicated for 10 s in toluene, and then washed with ethanol and DMF. The bromo-terminated wafers were placed in saturated NaN₃ in DMF at 20 °C for 48 h to get the azide-terminated surface. After being rinsed by DMF and H₂O and dried by N₂ flow, the wafers were stored in individual fluoroware containers and prevented from heat and light before being used.

Conjugation of Oligonucleotides with the Azide-Terminated Silicon Substrates via Click Reaction. CuSO₄–TBTA (1:1) ligand complex (0.03 mL of a 20 mmol stock solution in H₂O/DMSO/*t*-BuOH 4:3:1), tris(carboxyethyl)phosphine (TCEP; 0.03 mL of a 20 mmol stock solution in water), 0.04 mL of H₂O, and 0.08 mL DMSO were added into the single-stranded oligonucleotide (22 μ M) solution. Then the azide-terminated silicon wafer was immersed in this solution, which was continuously shaken gently for several hours (for ODN-2 to ODN-5: 20 h; for ODN-6 and 72 h) at 20 °C to accomplish the DNA immobilization and assembly. After that, the surface was successively washed by H₂O, ethanol, *n*-hexane, and finally by H₂O again to ensure that all unbound DNA and other reactants and catalysts were removed thoroughly from the surface. Then it was dried by N₂ flow and studied by AFM.

Hybridization of ODN-7 Probes to Complementary Targets. To a 1:1 CuSO₄–TBTA ligand complex (0.03 cm³ of a 20 mM stock solution in H₂O/DMSO/*t*-BuOH 4:3:1), tris(carboxyethyl)phosphine (TCEP; 0.03 cm³ of a 20 mM stock solution in water), 0.04 cm³ of H₂O, and 0.08 cm³ of DMSO were added. The single-stranded oligonucleotide (22 μ M) ODN-7 in 250 μ L of a 1 M NaCl solution was annealed by heating the solution at 80 °C for 5 min followed by slow cooling. This oligonucleotide solution was added to the above solution. Then the azide-terminated silicon wafer was immersed in this solution and shaking was continued slightly for several hours at 20 °C. The DNA-immobilized surface was washed with deionized H₂O, ethanol, *n*-hexane, and finally deionized H₂O to ensure that all unbound DNA and unreacted catalyst were removed from the surface. Then the surface was thoroughly dried under a flow of N₂ gas and investigated by AFM. Other experimental details can be found in the SI.

Acknowledgment. H.X. and G.Q. contributed equally to this work. The authors T.S. and G.Q. thank the Chang Jiang Scholars Programme of Chinese Ministry, the Alexander von Humboldt Foundation, and the Federal Ministry of Education and Research of Germany (Sofja Kovalevskaja Award project) for funding; F.S. and H.X. appreciate financial support by ChemBiotech, Münster, Germany. We thank Mrs. Jessica Guddorf in Muenster University for her help in the DLS experiment.

Supporting Information Available: Experimental details, large-scale AFM images, MALDI-mass spectra of oligonucleotides. This material is available free of charge via the Internet at <http://pubs.acs.org>.

JA105246B

(21) (a) Longo, G.; Girasole, M.; Pompeo, G.; Cricenti, A.; Andreano, G.; Cattaruzza, F.; Cellai, L.; Flamini, A.; Guarino, C.; Prosperi, T. *Biomol. Eng.* **2007**, *24*, 53. (b) Rasched, G.; Ackermann, D.; Schmidt, T. L.; Broekmann, P.; Heckel, A.; Famulok, M. *Angew. Chem., Int. Ed.* **2008**, *47*, 967.